

## Abstract

The ability to protect modern infrastructure as effectively as possible from lightning strikes has become essential with the development of complex electronic, communication, and power systems (Riouset, 2010). In order to determine the most effective geometry of a lightning rod, one must first understand the physical difference between their current designs. Benjamin Franklin's original theory of sharp tipped rods suggests an increase of local electric field, while Moore et al.'s (2000) studies of rounded tips evince an increased probability of strike (Moore et al., 2000; Gibson et al., 2009). The beginning of the connection process between the descending lightning channel and the upward connecting leader, there is the formation of a "precursor" plasma discharge around the rod in the form of an ionization front (Golde, 1977). In this analysis, the plasma discharge is produced between two electrodes with a high potential difference, resulting in ionization of the neutral gas particle and creating a current in a gas medium. This process, when done at low current and low temperature, creates a corona, or "glow" discharge, which can be observed as a luminescent emission. The Cartesian geometry known as Paschen, or Townsend, theory is particularly well suited to model experimental laboratory scenario, however, it is limited in its applicability to lightning rods. Franklin's sharp tip and Moore et al.'s (2000) rounded tip fundamentally differ in the radius of curvature of the upper end of the rod. As a first approximation, the rod can be modelled as an equipotential conducting sphere above the ground. Hence, we expand the classic Cartesian geometry into a spherical geometry, where a small radius effectively represents a sharp tip rod, while larger, centimeter-scale radius represents a rounded, or blunt tip. Empirical investigations of lightning-like discharge are of a limited size. They are typically either a few meters in height, or span along the ground to allow the discharge to occur over a large distance. Yet, neither scenarios account for the change in neutral charge density, which conditions the reduced electric field, and therefore hardly reproduce the condition of discharge as it would occur under normal atmospheric conditions (Raiser, 1991). In this work we explore the effects of shifting from the classical parallel plate analysis to spherical and cylindrical geometries more adapted for studies of lightning rods. Utilizing Townsend's equation for corona discharge, we estimate a critical radius and minimum breakdown voltage that allows ionization of the air around a lightning rod. We solve the problem both numerically and analytically to present simplified formulas for each geometry, and discern a definitive effective design. The development of a numerical framework will ultimately let us test the influence of parameters such as background ionization, initiation criterion, and charge conservation on the values of the critical radius and minimum breakdown voltage.

## I. Introduction



Figure 1: Glow Coronas form on the edges of a powerline transformer (Berkoff, 2005).

### Corona Discharge

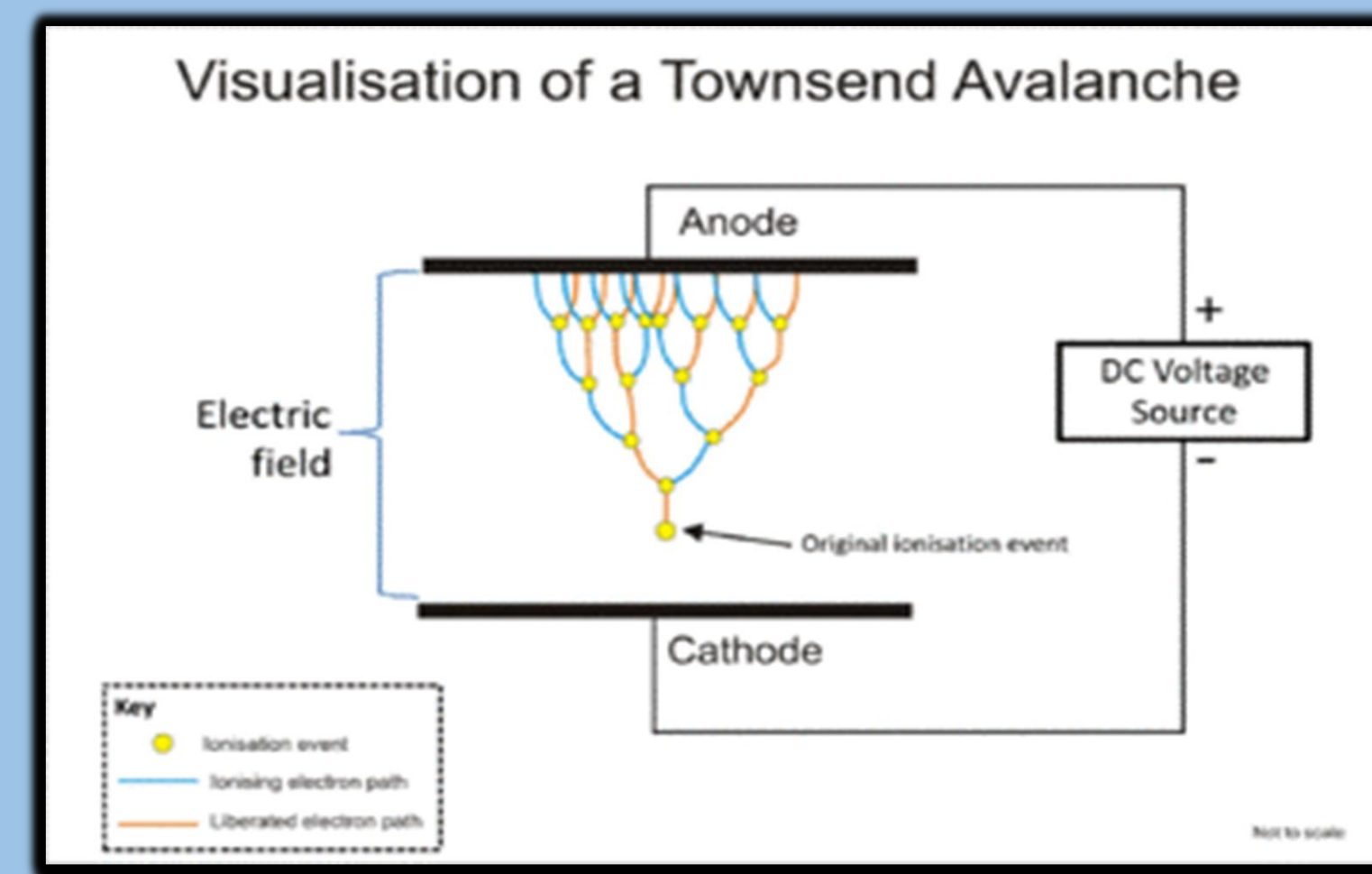
- Type of discharge around a conductor caused by an electric field;
- Weakly ionized gas responsible for glow at visible wavelengths;
- Hypothesized to promote the formation of upward connecting leaders in lightning discharges

### Electron Avalanche

The process of electron avalanching is similar between various types of discharges:

- Initial step of a discharge;
- Displace one or more electrons with enough kinetic energy to displace other electrons;
- Avalanche criteria =  $\ln(Q)$ ;  $Q = 10^4 \approx 18-20$ .

Figure 2: → A visual representation of the process of an electron avalanche in Townsend's breakdown model. This can also be referred to as a Cartesian case due to the parallel plate structure (Gewartowski et al., 1965).



### Types of Discharges

The three types of discharge can be thought as different levels of energy and temperature; with Corona as the weakest and leader being the strongest.

Parameter	Glow Corona	Streamer	Leader
Temperature	~300 K	~300 K	>5000 K
Electron energy	1-2 eV	5-15 eV	1-2 eV
Electric field	0.2-2.7 kV/cm	5-7.5 kV/cm	1-5 kV/cm
Electron density	$2.6 \times 10^8 \text{ cm}^{-3}$	$5 \times 10^{13}-10^{15} \text{ cm}^{-3}$	$4 \times 10^{14} \text{ cm}^{-3}$

Table 1: Characteristics for types of plasma discharge at sea level [Adapted from (Gibson et al, 2009)].

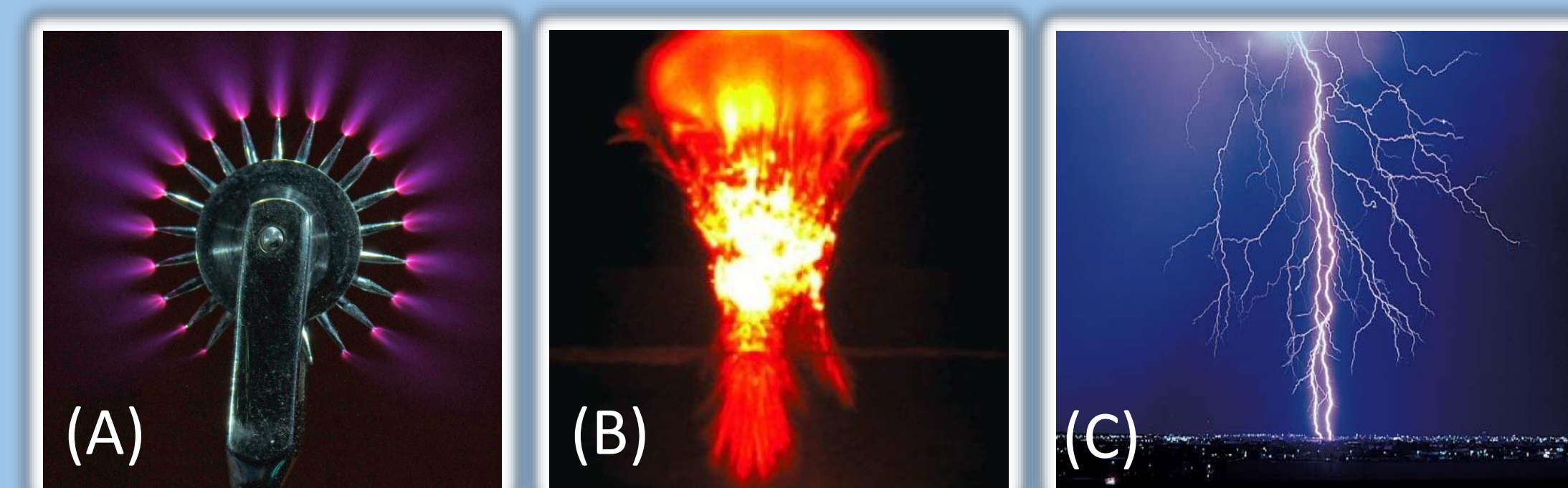


Figure 3: (A) A Wartenberg wheel in which glow Coronas form at the tip of each spindle. (Berkoff, 2005); (B) Streamers are the origin of a sprite phenomenon (courtesy of H. H. C. Stenbaek-Nielsen); (C) A lightning strike is perhaps the most common example of a leader discharge. (Whetmore, 2016).



Figure 4: Photograph of six blunt aluminum rods, each of which has been struck by lightning on South Baldy Peak (Moore et al., 2003).

## Objectives

- Understand effects of different geometries on Paschen Theory;
- Develop numerical models for Cartesian and spherical geometries;
- Discern the differences between sharp or blunt tipped rods for corona discharge;
- Estimate critical radius at Stoletov's point.

## Paschen Theory

- Minimum breakdown voltage for two parallel plates;
- $\alpha_{eff}(E) = \frac{v_i(E) - v_a(E)}{\mu_e(E)E} \approx Ape^{\left(\frac{-Bp}{E}\right)}$
- Stoletov's point:  $\frac{\partial V}{\partial x} = 0$ ;
- Analytical solution for a Cartesian case such as in Figure 2.

## II. Model Formulation

- $\nabla E = \rho_0 = 0$
- $E(R_1) = E(c) = E_c \approx 28 \frac{N_0}{N} \text{ kV/cm}$
- $p = Nk_B T$
- $A = 7.7 \frac{1}{\text{cm} \cdot \text{Torr}}$
- $B = 274.7 \frac{V}{\text{cm} \cdot \text{Torr}}$

Geometry	Analytical Solution	Numerical
Cartesian	<ul style="list-style-type: none"> <li>• <math>\int_{x_1}^{x_2} \alpha_{eff} dx = \ln(Q)</math></li> <li>• <math>x_1 = 0</math></li> <li>• <math>\alpha_{eff}(E) = Ape^{\left(\frac{-Bp}{E}\right)}</math></li> <li>• <math>d = x_2 - x_1</math></li> <li>• <math>\frac{\partial V}{\partial d} = 0</math>: Stoletov's point</li> </ul>	<ul style="list-style-type: none"> <li>• <math>\int_{x_1}^{x_2} \alpha_{eff} dx = \ln(Q)</math></li> <li>• <math>x_1 = 0</math></li> <li>• <math>\alpha_{eff}(E) = \frac{v_i(E) - v_a(E)}{\mu_e(E)E}</math></li> <li>• <math>d = x_2 - x_1</math></li> <li>• <math>\frac{\partial V}{\partial d} = 0</math>: Stoletov's point</li> </ul>
Spherical	<ul style="list-style-type: none"> <li>• <math>\int_{R_1}^{R_2} \alpha_{eff} dr = \ln(Q)</math></li> <li>• <math>R_2 \rightarrow \infty</math></li> <li>• <math>\alpha_{eff}(E) = Ape^{\left(\frac{-Bp}{E}\right)}</math></li> <li>• <math>\frac{\partial V}{\partial R_1} = 0</math>: Stoletov's point</li> </ul>	<ul style="list-style-type: none"> <li>• <math>\int_{R_1}^{R_2} \alpha_{eff} dr = \ln(Q)</math></li> <li>• <math>R_2 \rightarrow \infty</math></li> <li>• <math>\alpha_{eff}(E) = \frac{v_i(E) - v_a(E)}{\mu_e(E)E}</math></li> <li>• <math>\frac{\partial V}{\partial R_1} = 0</math>: Stoletov's point</li> </ul>

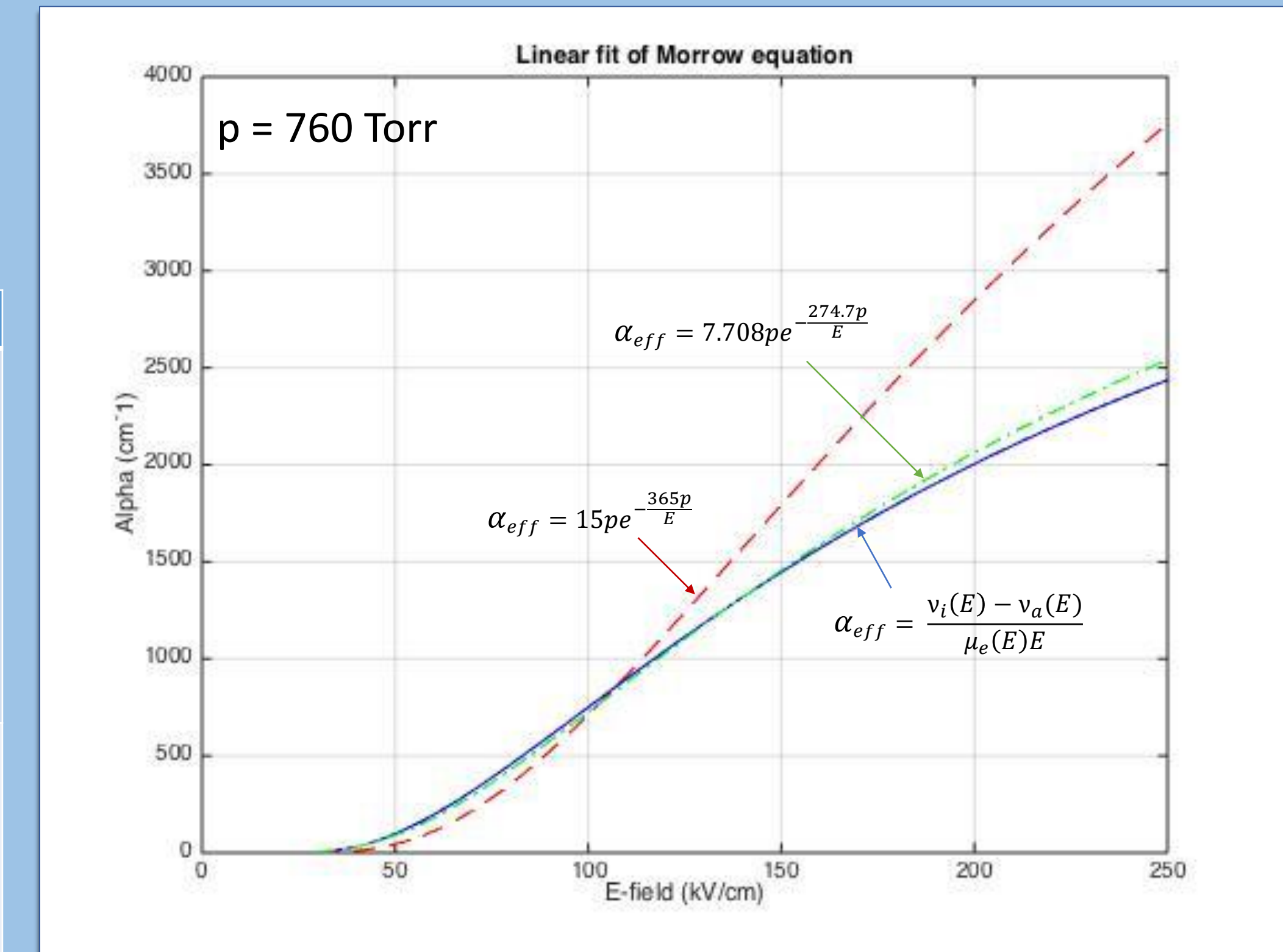


Figure 5: The exponential fit model of the exponential approximation provided by Townsend and the equation  $\int_{R_1}^{R_2} \alpha_{eff} dr = \ln(Q)$  given by Morrow and Lowke (1997).

## III. Results and Discussion

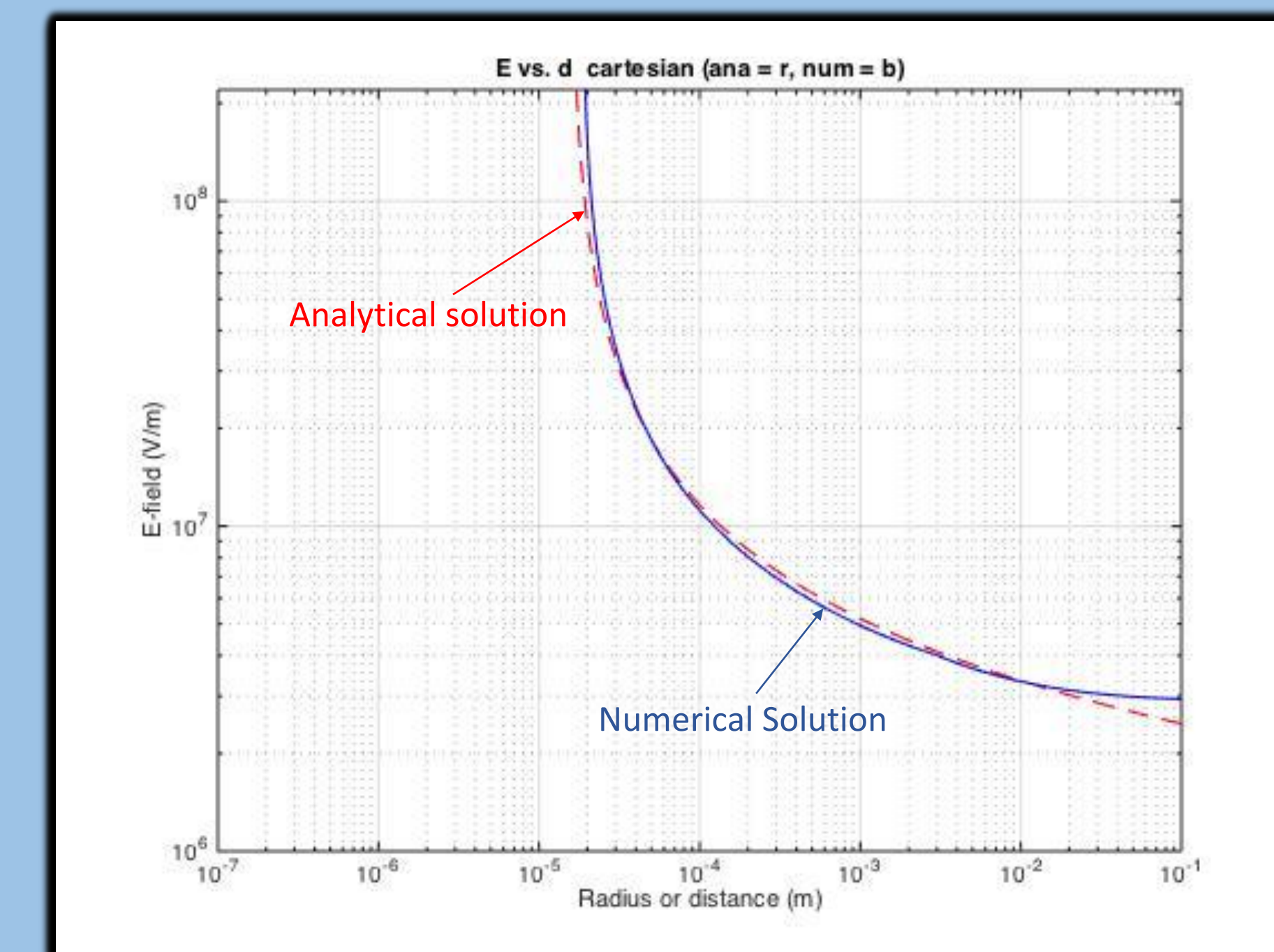


Figure 6: Analytical solution for electric field ( $E$  vs.  $d$ ) as a function of  $d$  in Cartesian geometry:

$$E(d) = \frac{-Bp}{\ln\left(\frac{\ln(Q)}{Apd}\right)}$$

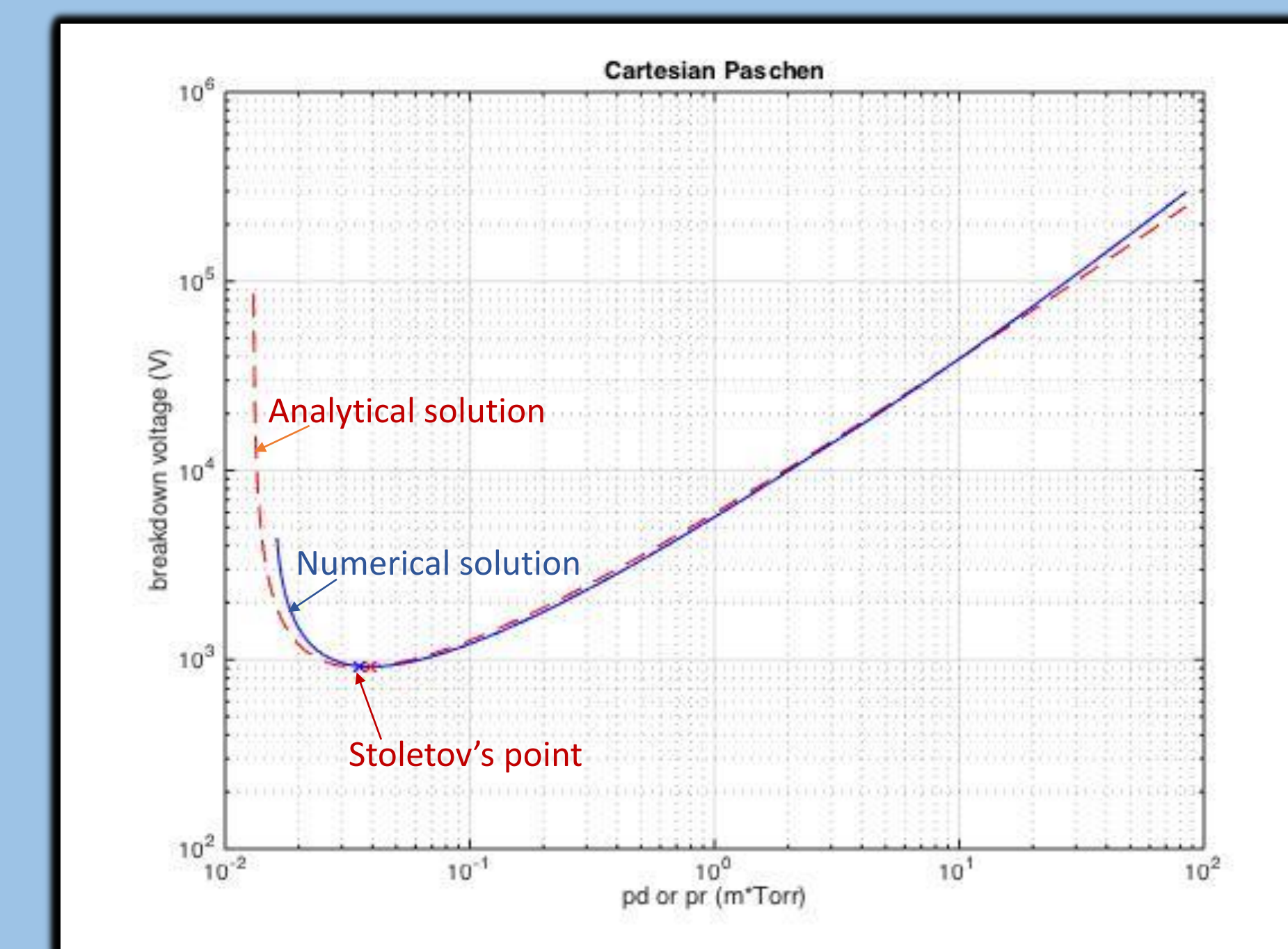


Figure 7: Paschen curve for Cartesian geometry:

- Analytical solution:  $V(d) = \frac{-Bpd}{\ln\left(\frac{\ln(Q)}{Apd}\right)}$
- Stoletov's point:  $V_{min} = \frac{eB}{A} \ln(Q)$ .

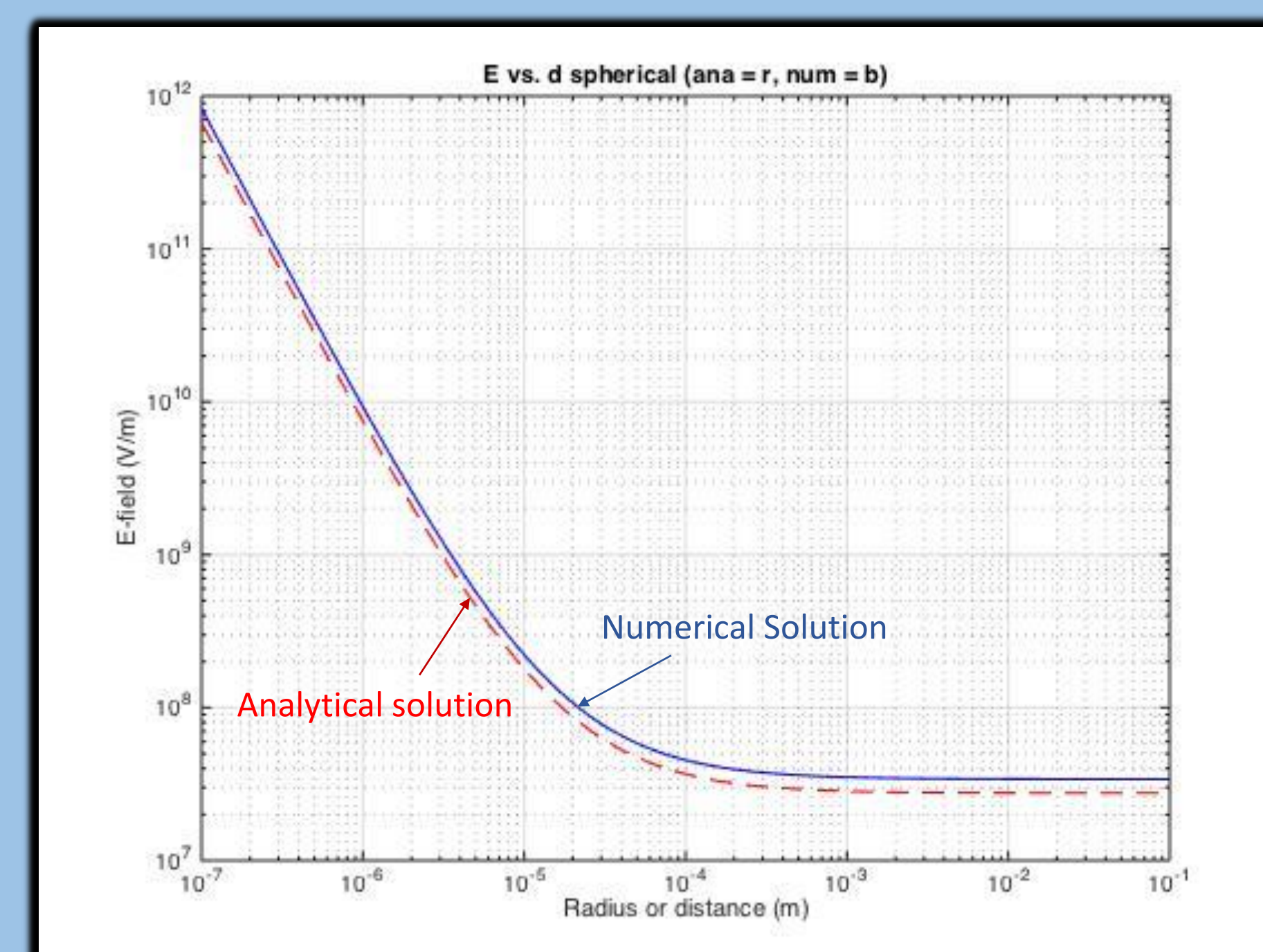


Figure 8: Analytical solution for electric field ( $E$  vs.  $d$ ) as a function of  $r_1$  in Spherical geometry:

$$E(r) = \frac{4B(\ln(Q) + ApR_1)^2}{\pi p A^2 R_1^2}$$

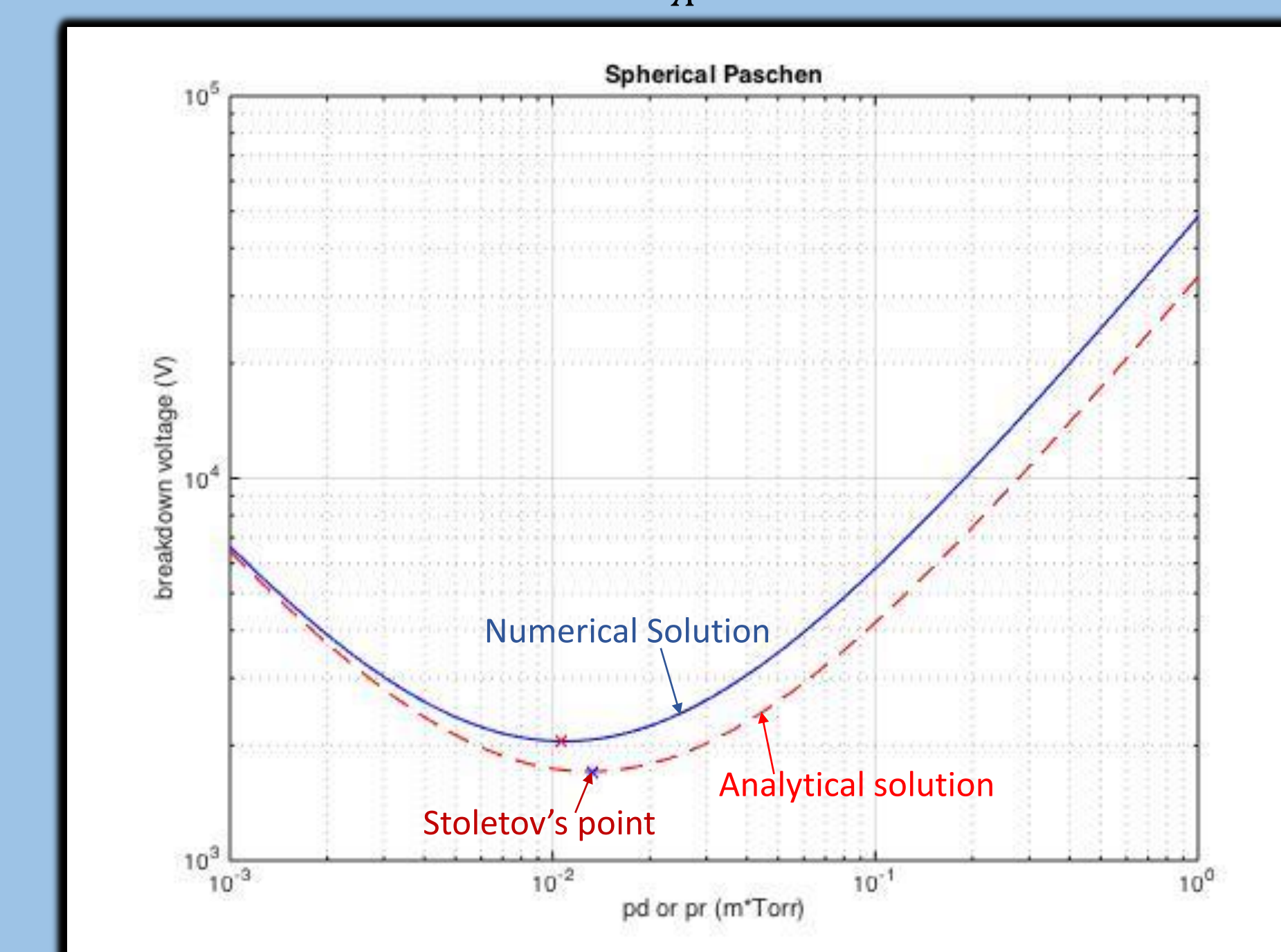


Figure 9: Paschen curve for spherical geometry:

- Analytical solution:  $V(r) = \frac{4B(\ln(Q) + ApR_1)^2}{\pi p R_1}$
- Stoletov's point:  $V_{min} = \frac{16B}{\pi A} \ln(Q)$ .

A comparison of the two geometries illustrates the similarities and differences, as well as the need for modern models for the considered geometries in which Corona discharges form.

Similarities	Differences
<ul style="list-style-type: none"> <li>• Paschen curves for both cases converge for large values of <math>r</math>, in which spherical geometry would behave similar to a parallel plate configuration;</li> <li>• Values of Critical radius (<math>R_c</math>), electric field (<math>E</math>), and breakdown voltage (<math>V_{min}</math>) at Stoletov's point, the difference being a ratio of <math>\frac{16\pi}{e}</math>.</li> </ul>	<ul style="list-style-type: none"> <li>• Both analytical and numerical solutions for Stoletov's point match for Cartesian geometry (Paschen's classical theory);</li> <li>• In spherical geometry the analytical and numerical solutions for Stoletov's point are noticeably different.</li> </ul>

Table 2: Highlights of the key similarities and differences between the two geometries.

## IV. CONCLUSIONS

The results and conclusions obtained in this work can be summarized as follows:

- The importance of Corona discharge in the formation of upward leaders makes its understanding fundamental to assess the effectiveness of lightning rod designs;
- Our models provide analytical formulas as well as numerical solutions that allow estimates of the critical radius and minimum breakdown voltage for Corona discharge in Cartesian and spherical geometries;
- Our revised A and B coefficients in the exponential fit of  $\alpha_{eff}$  improve the match between the analytical and numerical solutions in both geometries;
- To improve these estimates, models will be further improved by the implementation of other factors such as the presence of space charges (background ion density);
- Our calculations of the critical E-field remain above the generally accepted values for initiation of Corona discharges; hence more work is needed.